



Behaviors of Precast Reinforced Concrete Drainage Pipes under Static Load Using Finite Element Model

Narongsak Kosaiyakanon^{1,2}, Chaisak Pisitpaibool^{1*}

¹Department of Civil Engineering, Thammasat School of Engineering, Thammasat University, Pathumtani, THAILAND.

²Department of Rural Roads, Ministry of Transport, THAILAND.

*Corresponding Author (Tel: +669 2092 7094, Email: cha_xyz@hotmail.com).

Paper ID: 13A6P

Volume 13 Issue 6

Received 14 January 2022

Received in revised form 04 May 2022

Accepted 09 May 2022

Available online 18 May 2022

Keywords:

ABAQUS; Precast reinforced concrete drainage pipe (RCP); Reinforced concrete; TIS.128-2549; Circular pipe; Elliptical pipe; Finite element.

Abstract

This paper presents the behavior of the reinforced concrete drainage pipe (RCP) subjected to static loading conditions using a finite element model based on the standard No. TIS. 128-2549. For the first category, three types of circular prefabricated reinforced concrete pipes are investigated. These circular pipes include the single circular, the double circular, and the elliptical steel cages. The development of stresses in concrete and reinforcing bars obtained from the finite element model along the load-deflection curve of the circular pipes is sequentially presented. Similar to those found in literature, the redistribution process appears. Since the applied load is continuously increased in its magnitude, the excessive stress developed is transferred from the concrete to the reinforcing steel, whose strength capacity is better, especially for tension. For the second category, the circular pipes consisting of either circular or elliptical steel cages are compared with the elliptical pipes consisting of elliptical steel cages. For comparison, each pipe contains the same cross-sectional area. The load-deflection curves obtained from the circular and elliptical RCP present a similar behavior, however, it is different in their magnitude. The elliptical pipe with a vertical position provides the significantly highest ultimate load capacity. It confirms that any cross-sectional area of these vertical elliptical RCP provides the longest moment arm of the resisting moment.

Disciplinary: Civil Engineering & Technology.

©2022 INT TRANS J ENG MANAG SCI TECH.

Cite This Article:

Kosaiyakanon, N., Pisitpaibool, C. (2022). Behaviors of Precast Reinforced Concrete Drainage Pipes under Static Load Using Finite Element Model. *International Transaction Journal of Engineering, Management, & Applied Sciences & Technologies*, 13(6), 13A6P, 1-22. <http://TUENGR.COM/V13/13A6P.pdf> DOI: 10.14456/ITJEMAST.2022.121

1 Introduction

Drainage work is provided as an integral part of the transportation service to eliminate the excess surface water, especially from the rainfall which may cause damage to passenger traffic. A channel for draining or even a water channel can be included as one type of drainage work to get rid of the surface water out of the roads. An underground drainage system is a preferable selection due to the need for a wider traffic surface. This selection, however, increases the applied loads, which include not only the heavy truck weight transferring from the wheels to the traffic surface but also the above soil weight and the groundwater. Behaviors of the structural drainage system need to be investigated to confirm their survival under different stages of the combination of these loads. The finite element model is one of the popular procedures to simulate the structural behavior reducing time and cost consumption by laboratory experiments. The numerical analysis can capture the different stages of material response caused by the applied loads. This includes the development of stress distribution across a section of the complicated materials, such as the behavior of the reinforcing bar and concrete subjected to the load history based on the performance of the reinforced concrete drainage structure. Literature shows that some researchers use ABAQUS software to apply the finite element method for simulation of the RCP behavior using the three-edge-bearing (TEB) test method. Tehrani (2016) formulates the models to compare the difference between the single and double cage behavior of the RCP according to ASTM standards. Younis et. al. (2021) simulate the pipe models with three types of transverse reinforcement, which are single-cage, double-cage, and triple-cage. Ramadan et. al. (2020) creates the non-linear 3D FEM models of the RCP with a single elliptical steel cage to investigate the effect of the cage rotation on the reduction of the load and moment capacity of the pipe.

In Thailand, the load test for RCP is governed by AS/NZS 4058-2007 [30]. To evaluate the structural performance of pipes, the pipe and load orientation is performed similarly to the TEB test arrangement. However, the magnitudes of their size and load capability are different from the literature. In addition, the Thai specification does not require consideration of the elliptical concrete pipe. The development of Thailand's transportation system accelerates many large trucks, especially with heavy weight transmitted through the surface of the traffic. These overweights can affect and damage the road structures including the underground RCP behavior. The simulation of the structural performance and failure mechanisms of RCP obtained from the finite element model can be one of the guidelines to review and update the available RCP standard raising the infrastructure development and transport services. The objective of this study is to simulate the finite element models of the TEB test of the RCP for drainage work in Thailand certifying by the standard No.TIS.128-2549 from the Thai Industrial Standard (TIS). The finite element models are both the circular pipes and the pipes of elliptical cross-section. The first circular pipes include the single circular, the double circular, and the elliptical steel cages. The second pipes of elliptical cross-section consider the single elliptical and the double elliptical steel cages. In addition, the

cooperation between stress development in concrete and reinforcing steel is expected to propose in a simple systematic sequence according to the pipe performance during the load history.

2 Literature Review

Wen et al. (2016) tested reinforced concrete pipes (RCP) using the three-edge-bearing (TEB) method. Cracking was generally found first at the crown of the circular pipes. The test device for determining the tensile and compressive strength between the outer and inner pipe wall was determined by using bending tests of both concave and convex segments representing the curved beams. Different production process provides different concrete strength between the inner and outer pipe walls.

da Silva et al. (2018) tested RCP using a TEB method. Two types of RCP were identified in the test; spigot-pocket (SPP) and ogee joint pipes (OJP). Thirty-two pipes, with a nominal diameter of 800 and 1200 mm, were laboratory performed. The pipes were divided into two series, each of which consisted of 16 pipes. The testing method complied with the ASTM C76 (2016) and ABNT (2007). The pipe stiffness was increased by the presence of the pocket.

Tehrani (2016) conducted the uniaxial cylinder tests to verify the material properties for ABAQUS software to simulate the behavior of RCP under the TEB test. The graphs from the TEB tests were used to validate the proper work of the FEM simulation. Results obtained from the simulations indicated that the location of the circumferential reinforcements correlated with the service and ultimate D-loads.

Younis et al. (2021) evaluated the pipe design classes by proposing 3D finite-element models to represent the RCP structural performance. Three types of transverse reinforcement arrangement within the pipes were single-cage, double-cage, and triple-cage. The behavior of RCP models using ABAQUS was calibrated by comparison with laboratory test results. The parametric study was performed on developing the FEM models to clarify the influence of the different reinforcements concerning the areas, concrete cover, positioning, and yield strength.

Ramadan et al. (2020) simulated the behavior of precast concrete pipe with a single elliptical steel cage using non-linear 3D FEM models. The rotation of the elliptical cage reinforcement resulted in a reduction of the serviceability load and moment capacity of the pipe. For the observation at 10 mm deflection, from 0 to 90 degrees rotation the load capability was reduced to 83%. In addition, at 10 mm deflection, the non-symmetrical shape of the elliptical cage reinforcement reduced only 5.9% of the symmetrical elliptical shape.

3 Overview of Drainage Pipes Investigation

The behavior investigation of the RCP subjected to static loading conditions using the finite element model is divided into two series. The first series investigates three types of circular prefabricated tongue-groove pipes. These circular pipes include the single circular, the double circular, and the elliptical steel cages. The second series includes the pipes of elliptical cross-

section, which are considered into two types; (a) Single elliptical and (b) Double elliptical steel cages. General information concerning the investigation is as follows:

3.1 Circular Reinforced Concrete Pipes and TIS. 128-2549

A good quality product of a reinforced concrete pipe for drainage work in Thailand is certified by Standard No. TIS. 128-2549 from the Thai Industrial Standard (TIS). The precast reinforced concrete drainage pipes are divided into two categories: bell-spigot and tongue-groove pipes. However, this investigation concentrates only on the tongue-groove pipes. The standard inner diameters of the tongue-groove pipes are 0.30, 0.40, 0.60, 0.80, 1.00, 1.20, 1.50, 1.75, 2.00, 2.25 and 2.50 m. Three Edge Bearing (TEB) test is specified for determining the compressive strength and load-bearing capacity. In the TEB test (Figure 1), the pipe is supported at its lower part by two longitudinal bearing strips, which can be wood or hard rubber. The upper part of the pipe is loaded by another bearing rubber strip under a wood beam to simulate a uniformly distributed load along the pipe length.

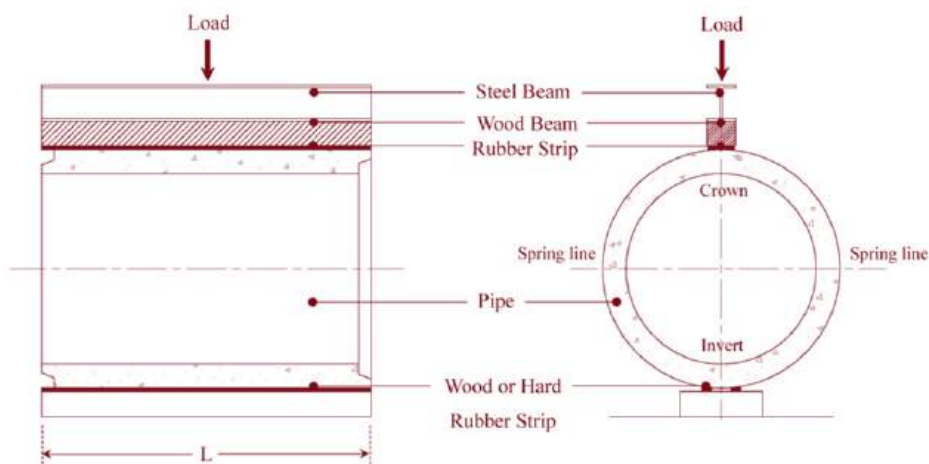
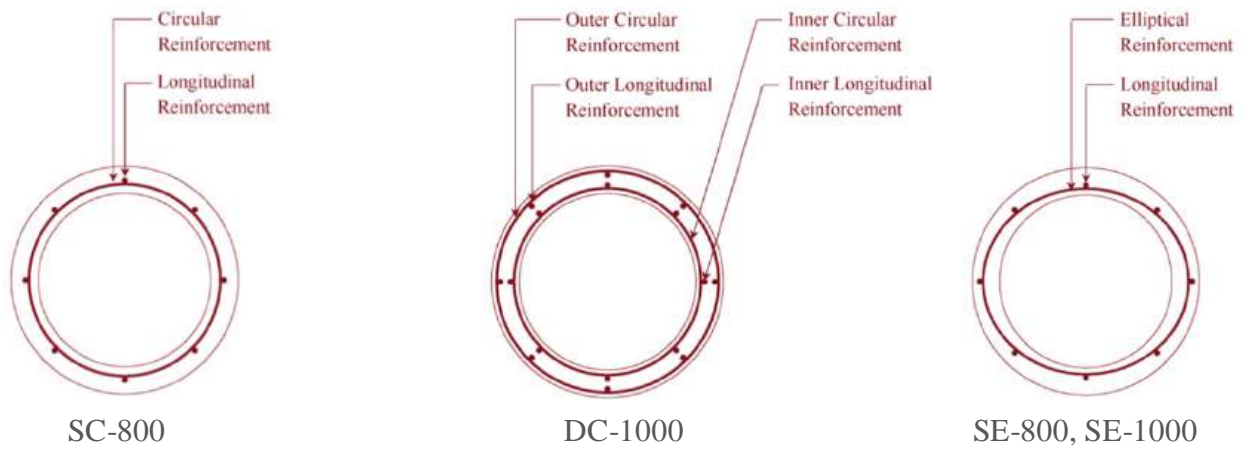


Figure 1: Set up of Three Edge Bearing Test according to TIS. 128-2549

In the first stage of this study, the circular tongue-groove pipes are considered into three types as shown in Figure 2; (a) Single circular, SC, (b) Double circular, DC, and (c) Single elliptical, SE, steel cages. Table 1 provides the general properties of the selected pipes for this study. This includes the pipe diameter, thickness, concrete strength, and the details of reinforcement. It shroud be noted that four specimens are selected in this stage; SC-800, DC-1000, SE-800, and SE-1000. The first two-letter indicates the configuration of the reinforcing bars. The following number indicates the inner diameter of the pipes. Tables 2, 3, and 4 provide the selected materials properties of concrete, steel, and wood for simulating the TEB test in FEM.

Table 1: Geometric properties of selected RCP.

Inner Diameter	Wall Thickness	Reinforcement		
		Circular		Elliptical Bar mm ² /m
mm	mm	Inner Bar mm ² /m	Outer Bar mm ² /m	
800	95	400 (RB6mm @ 70mm)	-	340 (RB6mm @ 80mm)
1000	110	420 (RB6mm @ 70mm)	320 (RB6mm @ 90mm)	470 (RB6mm @ 60mm)



(a) Single circular steel cage (b) Double circular steel cage (c) Single elliptical steel cage

Figure 2: Detail of the circular RCP in the first stage

Table 2: Material concrete properties

Item No.	Modulus of elasticity MPa	Poisson's Ratio	Density N/mm ³	Tensile strength MPa	Compressive strength MPa
Concrete	31,062	0.17	2.400x10 ⁻⁵	2.368	30

Table 3: Material properties of reinforcement

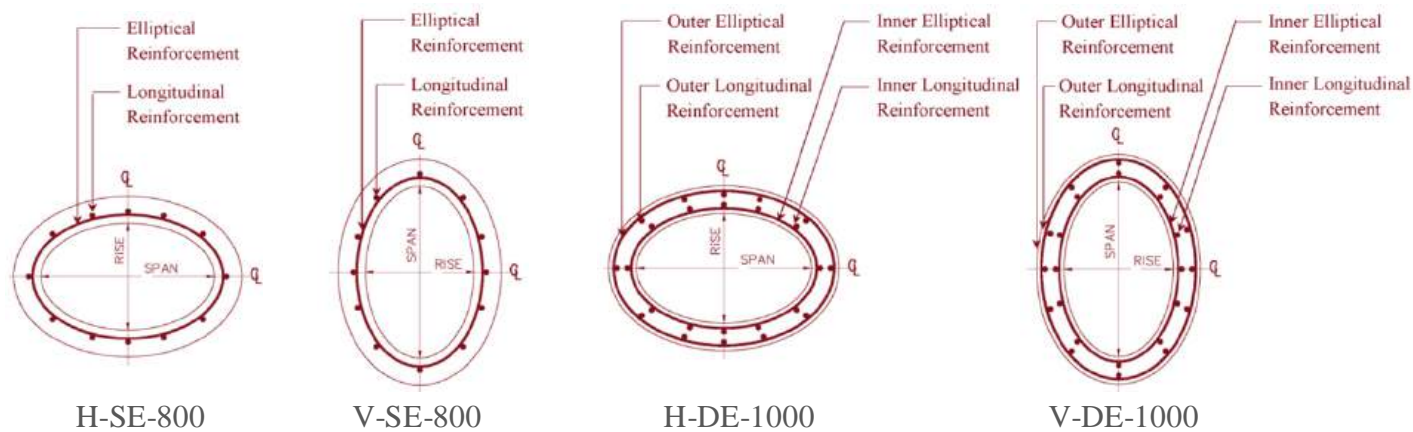
Item No.	Modulus of elasticity MPa	Poisson's Ratio	Density kg/m ³	Yield strength MPa, (kg/mm ²)	Tensile strength MPa, (kg/mm ²)
Reinforcement	200,000	0.30	7.850x10 ⁻⁵	235, (24)	385, (39)

Table 4: Material properties of wood

Item No.	Modulus of elasticity MPa	Poisson's Ratio	Density Kg/m ³
Wood	10,000	0.315	6.870x10 ⁻⁶

3.2 Elliptical Reinforced Concrete Pipe

In the second stage of this study, a comparison of the load-deflection behavior between the tongue-groove pipes of circular and elliptical cross-sections is investigated. Three types of circular RCP are obtained from the first stage. However, the pipes of elliptical cross-sections are considered into two types; (a) Single elliptical and (b) Double elliptical steel cages. The cross-section of the elliptical pipe is selected based on the Span/Rise ratio equal to 1.55 and resulting in the equivalent areas corresponding to the two types of circular pipes with single elliptical, SE-800, and double elliptical, DE-1000, steel cages. For comparison, the pipes of elliptical cross-section require two configurations, which are horizontal and vertical positions. In conclusion, four specimens for the pipes of the elliptical cross-section are needed in this stage as shown in Figure 3; H-SE-800, V-SE-800, H-DE-1000, and V-DE-1000. The first letter indicates the configuration of the pipes of the elliptical cross-section. The following letters and numbers indicate the configuration of the reinforcing bars and the inner diameter of the pipes, respectively. Table 5 provides the general properties of the pipes of the elliptical cross-section for simulating the TEB test in FEM.



(a) Single elliptical steel cages

(b) Double elliptical steel cages

Figure 3: Detail of the precast reinforced concrete elliptical drainage pipe.

Table 5: Geometric properties of FE models.

Circular	Elliptical	
Inner Diameter Mm	Inner Rise mm	Inner Span mm
800	670	1055
1000	864	1346

3.3 Typical Outcomes from Investigation

The typical outcomes of this investigation are the load-deflection relationship and the stress resultants obtained from the finite element simulation of the TEB test on the drainage pipes. The ratio of the vertical deflection, Δ , to the vertical inner pipe diameter under the applied loads is expressed in the percentage of deflection (δ) as

$$\delta(\% \text{ of diameter}) = \frac{\Delta}{\text{Vertical Inner Diameter}} \times 100\% \quad (1).$$

where: Δ = vertical deflection of RCP in millimeter.

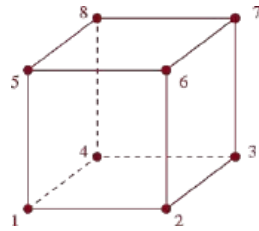
Based on the internal stress pattern obtained by the applied load, the pipe cross-sectional area can be divided by two shear lines into four segments. For the crown and invert, which are the top and bottom segments, the compressive and tensile stresses are produced in the outer and inner parts of the half-pipe thicknesses, respectively. For the two spring lines, one on the left and another one on the right, the compressive and tensile stresses are reversed as they are produced in the inner and outer parts of the half-pipe thicknesses, respectively.

4 Element Types and Material Properties

The TEB test of the RCP is simulated by creating the finite element model using ABAQUS software. The selection of the element types and application of the material properties to the model components are mentioned in the following subsections.

4.1 Element Types

Two element types are selected for modeling the RCP, which are solid and truss elements. The 3D solid element C3D8R, see Figure 4, is selected to model the concrete pipe and the bearing strips.



(a) 8-node brick solid elements



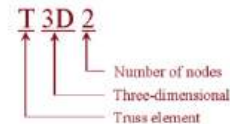
(b) How solid elements are called in Abaqus

Figure 4: Solid element (C3D8R)

The 3-dimensional truss element T3D2, as shown in Figure 5, is selected to model the reinforcing bar in terms of the steel cage of the precast RCP.



(a) 2-node straight truss element



(b) How truss elements are called in Abaqus

Figure 5: Truss elements (T3D2)

4.2 Material Properties

Three different material properties for finite element analysis to simulate the TEB test of the RCP model are defined depending on the three main components; which are concrete pipe, steel cage, and bearing strips. The behavior of the longitudinal bearing strips is simply defined by using the material properties of wood, as shown in Table 4. However, since the behavior of the RCP structure is nonlinear, the material properties of the steel cage and concrete pipe are rather complicated to define.

4.2.1 Steel Material

The material property of the steel cage of the RCP model is simulated as an elastic-plastic behavior. The stress-strain relationship for steel in tension and in compression is assumed to be identical, see Figure 6. The properties of the steel reinforcement are provided in Table 3. This includes yielding stress, $f_y = 235$ MPa, modulus of elasticity, $E_s = 200$ GPa, and Poisson's ratio, $\nu = 0.3$.

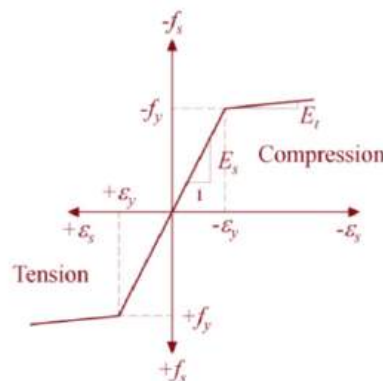


Figure 6: Elastic-plastic idealization

4.2.2 Concrete Material

The concrete damaged plasticity (CDP) model of ABAQUS software is selected to represent the material property of concrete. Information obtained from the stress-strain diagrams of

concrete including the inelastic region for both compression and tension behavior, see Figure 7, is required to create the CDP material model. The algorithms presented by Alfarah et al. (2017) are applied to develop the information obtained from the inelastic compressive and tensile stress-strain responses for modeling the concrete material.

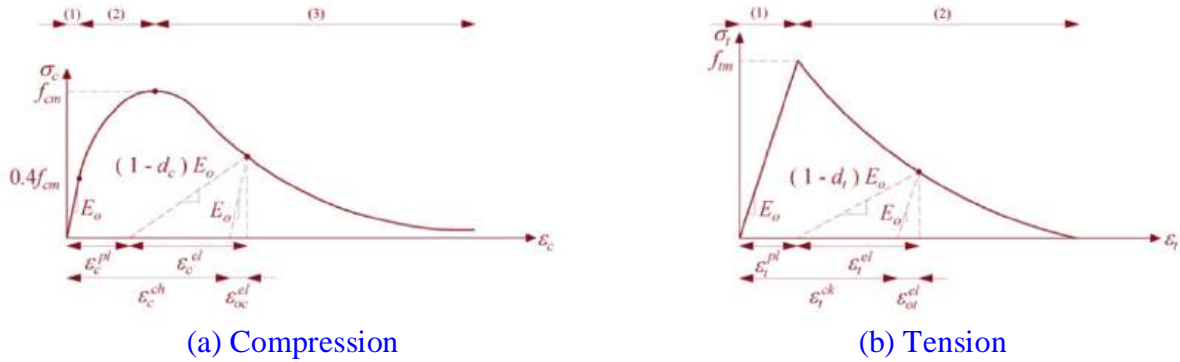


Figure 7: Uniaxial stress-strain diagram of concrete behavior

1) The values of the stress-strain relationship of concrete for compression behavior are divided into three parts, as shown in Figure 7(a). They are presented by Equations (2), (3), and (4), respectively.

$$\sigma_{c(1)} = E_0 \varepsilon_c \quad (2),$$

$$\sigma_{c(2)} = \frac{E_{ci} f_{cm} \left(\frac{\varepsilon_c}{\varepsilon_{cm}} \right)^2}{1 + \left(E_{ci} f_{cm} - 2 \right) \frac{\varepsilon_c}{\varepsilon_{cm}}} f_{cm} \quad (3),$$

$$\sigma_{c(3)} = \left(\frac{2 + \gamma_c f_{cm} \varepsilon_{cm}}{2 f_{cm}} - \gamma_c \varepsilon_c + \frac{\varepsilon_c^2 \gamma_c}{2 \varepsilon_{cm}} \right)^{-1} \quad (4).$$

2) The values of the stress-strain relationship of concrete for tension behavior are divided into two parts, as shown in Figure 7(b). They are presented by Equations (5), and (6), respectively.

$$\sigma_{t(1)} = E_0 \varepsilon_t \quad (5),$$

$$\sigma_{t(2)} = \frac{\sigma_1(W)}{f_{tm}} = \left[1 + \left(c_1 \frac{W}{W_c} \right)^3 \right] e^{-c_2 \frac{W}{W_c}} - \frac{W}{W_c} (1 + c_1^3) e^{-c_2} \quad (6).$$

3) The parameters in the Equations (2) to (6), such as f_{cm} , f_{tm} , E_0 , g_t , g_c and W_c , are computed from the Equations (7) to (13), respectively.

$$\text{Compressive stress strength, } f_{cm} = f_{ck} + 8 \quad (7),$$

$$\text{Tensile stress strength, } f_{tm} = 0.3016 f_{ck}^{\frac{2}{3}} \quad (8),$$

The initial tangent modulus of deformation of concrete,

$$E_{ci} = 10000 f_{cm}^{\frac{1}{3}} \quad (9),$$

$$\text{The undamaged modulus of deformation, } E_0 = E_{ci} \left(0.8 + 0.2 \frac{f_{cm}}{88} \right) \quad (10),$$

$$\text{The fracture (N/mm), } G_F = 0.073 f_{cm}^{0.18} \quad (11),$$

$$\text{Crushing energy (N/mm), } G_{ch} = \left(\frac{f_{cm}}{f_{tm}} \right)^2 G_F \quad (12),$$

$$\text{Critical crack opening, } W_c = 5.14 G_F / f_{tm} \quad (13).$$

4) The additional parameters in Equations (5) and (6), such as G_{ch} and ε_t which are presented for only the tension behavior, are calculated by Equations (14) and (15).

$$G_{ch} = \left(\frac{f_{cm}}{f_{tm}} \right)^2 G_F \quad (14),$$

$$\varepsilon_t = \varepsilon_{tm} + W/l_{eq} \quad (15).$$

5) The additional parameters, such as the specified concrete compressive strength f_{ck} , and the mesh size l_{eq} , are suggested to set up the initial assumption by using $b = 0.9$ and compressive stress strength, $\varepsilon_{cm} = 0.0022$.

The points in the stress-strain diagram of concrete for compression behavior obtained by substitution of a value of compressive strain ε_c into the appropriate Equations from (2) to (4). The corresponding compressive stress is then obtained. Repeat the procedure with different values of compressive strain to get different results of compressive stresses. The information can be plotted on the stress-strain diagram of concrete for compression behavior. The stress-strain diagram of concrete for tension behavior can be done by a similar procedure. Finally, all information can be input into the ABAQUS form for material properties to introduce the inelastic behavior into the finite element model.

For this study, the concrete compressive and tensile strength are specified as 30 MPa and 2.368 MPa, as shown in Table 2. The stress-strain diagrams of concrete including the inelastic region for both compression and tension behavior are obtained, as shown in Figure 8.

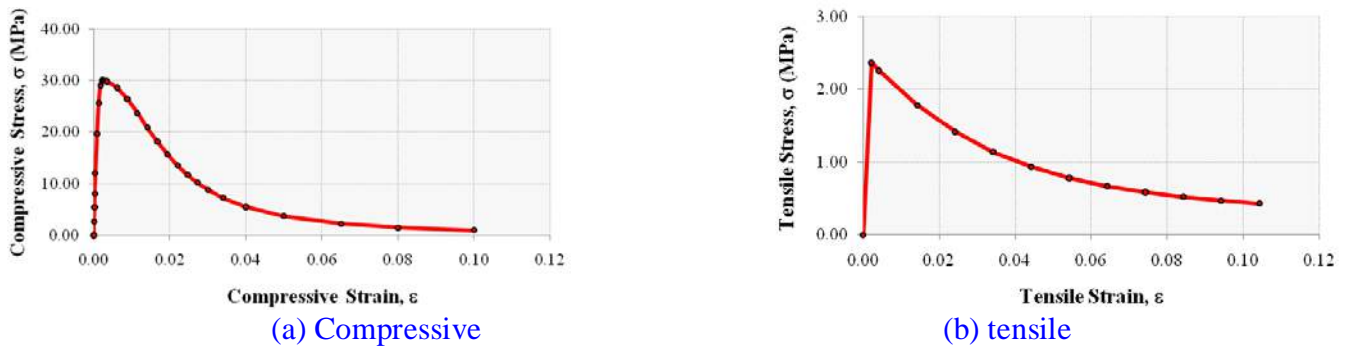


Figure 8: Stress-strain used to model concrete material

4.2.3 Other Concrete Plasticity Parameters

For the CDP model in ABAQUS, five plasticity parameters for concrete properties need to be defined. The values presented by Alfarah et al. (2017) are applied for this study, which are as follows:

1) **Dilation Angle (Ψ)**, This is the ratio of volume change to shear strain. The value of 36° is selected.

2) **Eccentricity**, This value is used to get a soft curvature of the potential flow and gives almost a similar dilation angle for a wide range of confining pressure values. An eccentricity of 0.1 is used.

3) σ_{bo}/σ_{co} **Parameter**, This is the ratio of the initial biaxial compressive strength to the uniaxial compressive strength. The default value of 1.16 is used.

4) **Viscosity Parameter**, This parameter is required when a convergence problem is caused by softening behavior. The viscosity parameter is assumed to be 0.001.

5) **Kc Parameter**, This parameter is determined by considering the yield surface in the deviatoric plane. Kc is the ratio of the second stress invariant on the tensile stress meridian (T.M.) to the second stress invariant on the compressive stress meridian (C.M.). The value 2/3 is used.

5 Finite Element Modeling

As a general finite element procedure, after assigning the material properties and meshing each component of the model, it needs to specify the interaction between elements of different components, boundary conditions, and load application to represent the test simulation and obtain the test results.

5.1 Components and Assemblage

Three main components, which are used to simulate the TEB test of the 3D RCP model, are shown in Figure 9. This includes the concrete pipe, the steel cage, and the (upper & lower) bearing strips. The geometric properties of the concrete pipe using solid element C3D8R and the steel cage using truss element T3D2 are presented in Table 1. In addition, the basic material properties of concrete, reinforcing bar, and wood bearing strip are provided in Table 2, 4, and 5, respectively.

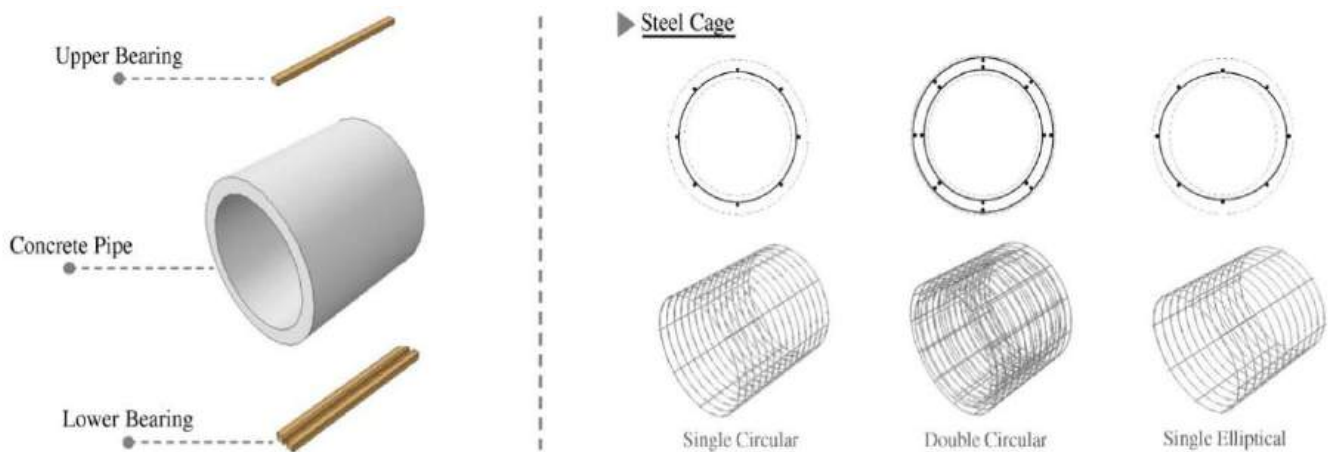


Figure 9: Parts and contact pairs in the FEM model

Figures 10, 11 and 12 show the assembly of the three main components of finite element models of the RCP with single circular, double circular, and single elliptical steel cages, respectively. These simulation models represent the TEB test method according to TIS. 128-2549. The bond interaction between the steel reinforcement and the concrete is developed by using the technique defined as the embedded region constraint. The steel (truss) element and the concrete (solid) element are defined as the embedded element and the host element, respectively. The

translational degrees of freedom of the embedded node are specified corresponding to the degrees of freedom of the host element.

The interaction between the concrete pipe and the bearing strips is obtained by applying the tie constraint to a pair of contact surfaces. By using this type of constraint, the active degrees of freedom of a pair of surfaces are specified to be equal. The contact surfaces of bearing strips and concrete are assigned to be the slave surfaces and the master surfaces, respectively.

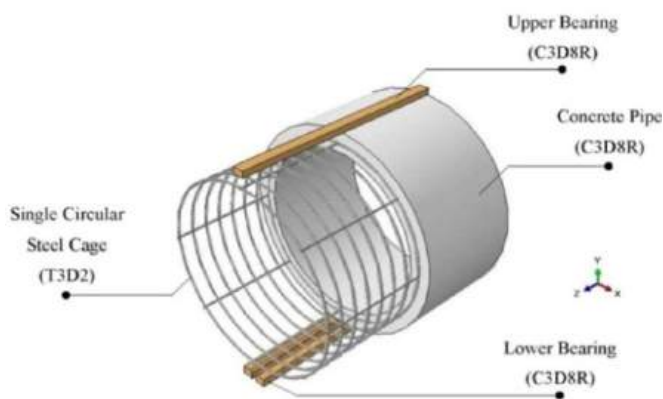


Figure 10: Components of finite element model of RCP with a single circular steel cage

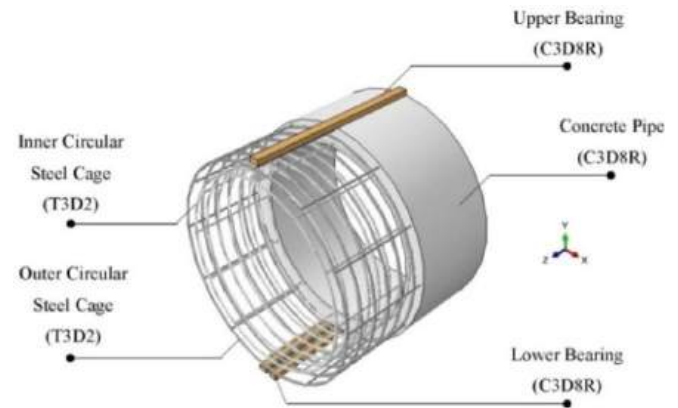


Figure 11: Components of finite element model of RCP with a double circular steel cage

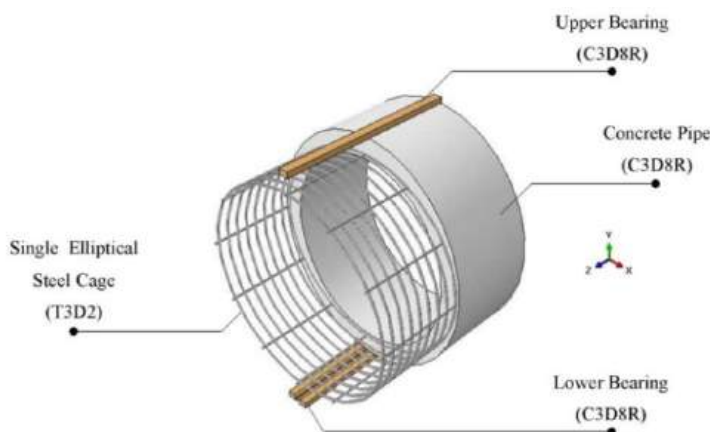


Figure 12: Components of finite element model of RCP with a single elliptical steel cage

5.2 Load and Boundary Conditions

A load applied on the top surface of the upper bearing strip is assigned by using a technique called a kinematic coupling constraint. This load is specified on a reference point located at a specific distance above the center of the top surface of the upper bearing strip. Using the coupling constraint locks all nodes on the top surface to the nodes at the reference point. The total response of all nodes on the top surface is equal to the response from the nodes of the reference point. The boundary conditions are set on nodes of the upper and lower bearing strips. To confirm that vertical movement can take place, the rollers are assigned to both sides along the length of the upper bearing strip. These rollers allow the upper bearing strip can move freely in the vertical (z) direction, however, the translational displacements in x- and y- directions are set to be zero. For the two-lower bearing strips, translational movement is not allowed. All translational displacements of the bottom surfaces of both lower bearing strips are set to be zero.

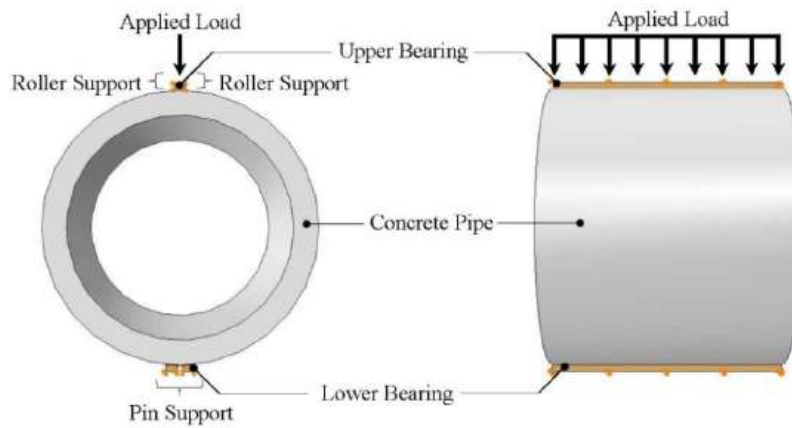


Figure 13: Specify boundary conditions and load

The static monotonic loading uses the displacement control technique. A vertical displacement is progressively applied in the downward direction on a reference point located above the top of the upper bearing strip up to failure to obtain the load-deflection curves of these RCP simulation models.

6 Results and Discussion

Results from the investigation of the RCP subjected to static loading conditions using the Finite Element model are divided into two categories. The first category presents the results obtained from the circular cross-sectional pipes with different types of steel cages. The second category compares the results obtained from the circular pipes with either circular or elliptical cages and the elliptical pipes with elliptical cages.

6.1 Circular Reinforced Concrete Pipes

For the first category, the load-deflection curves of the circular pipes with the single circular cage SC-800, the single elliptical cage SE-800, the double circular cage DC-1000, and the single elliptical cage SE-1000, are presented in Figures 14, 15, 16, and 17, respectively. In addition, the corresponding principal stress development, which is distributed across the cross-section of these circular pipes, is expressed in Tables 6, 7, 8, and 9, respectively. The letters in the first row refer to the corresponding points in the load-deflection curves repeated in the last row. The sequence of these letters refers to the increase in the magnitude of the applied load. The second and third rows are the stress development in concrete and circular reinforcing bar, respectively, generated on the pipe cross-sectional area. It should be noted that the color scale bars of concrete and reinforcing bar showing in the last row represent the different magnitude of stresses. The fourth and fifth rows present the magnifier of the stress development of the reinforcing bar near the crown (highest inside level), the invert (lowest inside level) and the spring-line (mid-height of the vertical level) of the pipe wall.

Under the TEB test simulation, the RCP exhibits similar behavior to a vertical ring subjected to a downward loading. The pipe diameter in the vertical direction tends to be decreased while in the horizontal direction tends to be increased. The pipe wall segment behaves similarly to a simply supported beam subjected to a point load. Therefore, at the crown or the highest level, the

compressive and tensile stresses are created above and below the neutral axis of the pipe wall. In contrast, at the invert or the lowest level, the compressive and tensile stresses are created below and above the neutral axis of the pipe wall. For the spring line level or the level of horizontal diameter, the compressive and tensile stresses are produced inward and outward in the radial directions from the neutral axis of the pipe wall. At point (a) of Tables 6 to 9, when the applied load is initially increased after the elastic deformation, the high-stress concentration in concrete starts to form at the crown, the invert, and the outer faces of the spring-lines. As the load is further increased, as shown at point (b) in Tables 6 to 9, the high principal stress in concrete spreads over the region at the location of stress concentration. In addition, the moderate stress in circumferential reinforcing steel begins to develop at the identical location of the stress concentration in concrete. For further increasing of the applied load within the inelastic range, as shown at points (c) to (f) in Tables 6 to 9, the stress in the steel bar increases continuously. This implies that the excessive principal stress carried by the concrete capability is transferred to the reinforcing steel bar.

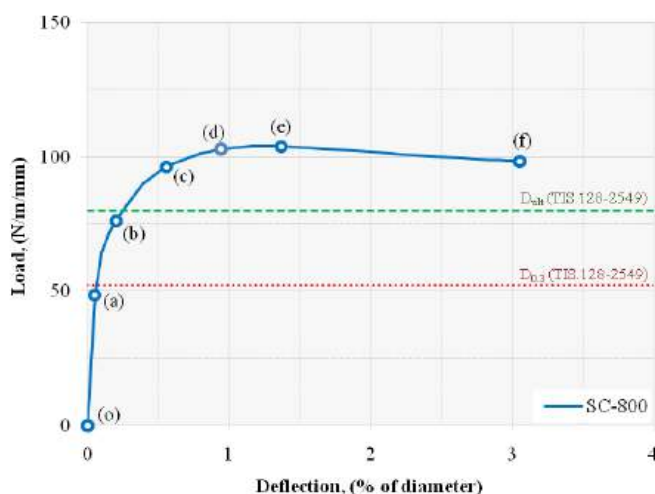


Figure 14: Load-deflection curves for typical SC-800 (circular pipe with single circular cage)

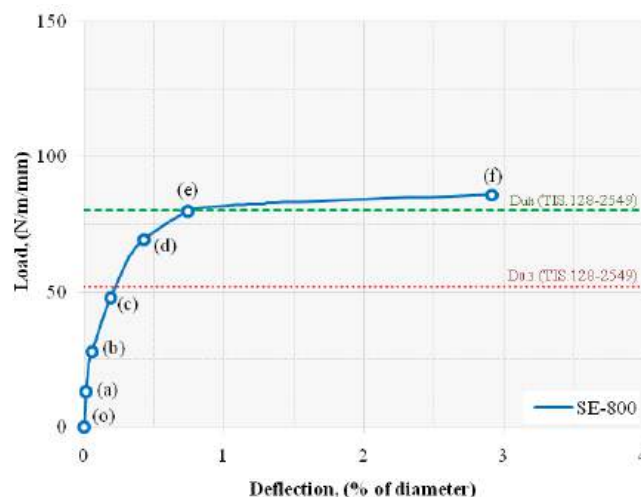


Figure 15: Load-deflection curves for typical SE-800 (circular pipe with single elliptical cage)

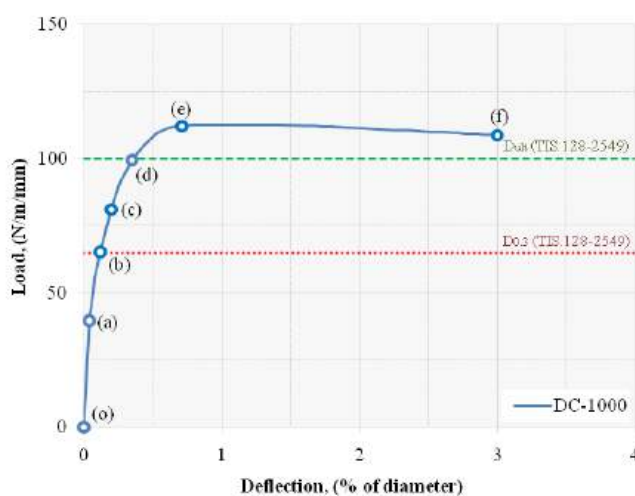


Figure 16: Load-deflection curves for typical DC-1000 (circular pipe with double circular cage).

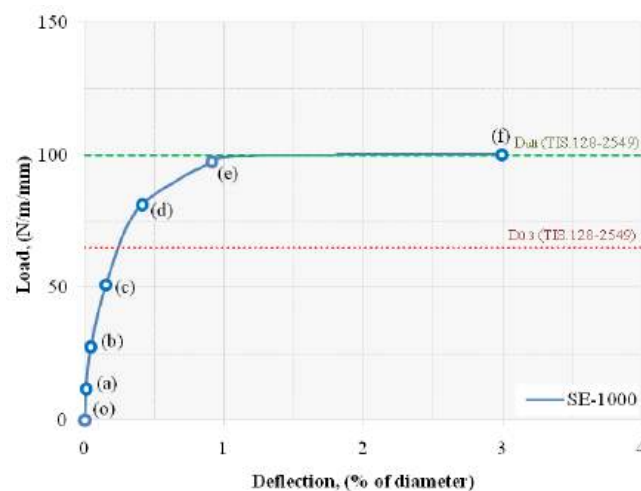


Figure 17: Load-deflection curves for typical SE-1000 (circular pipe with single elliptical cage)

Table 6: Development of stress distribution for typical SC-800 single circular steel cage model

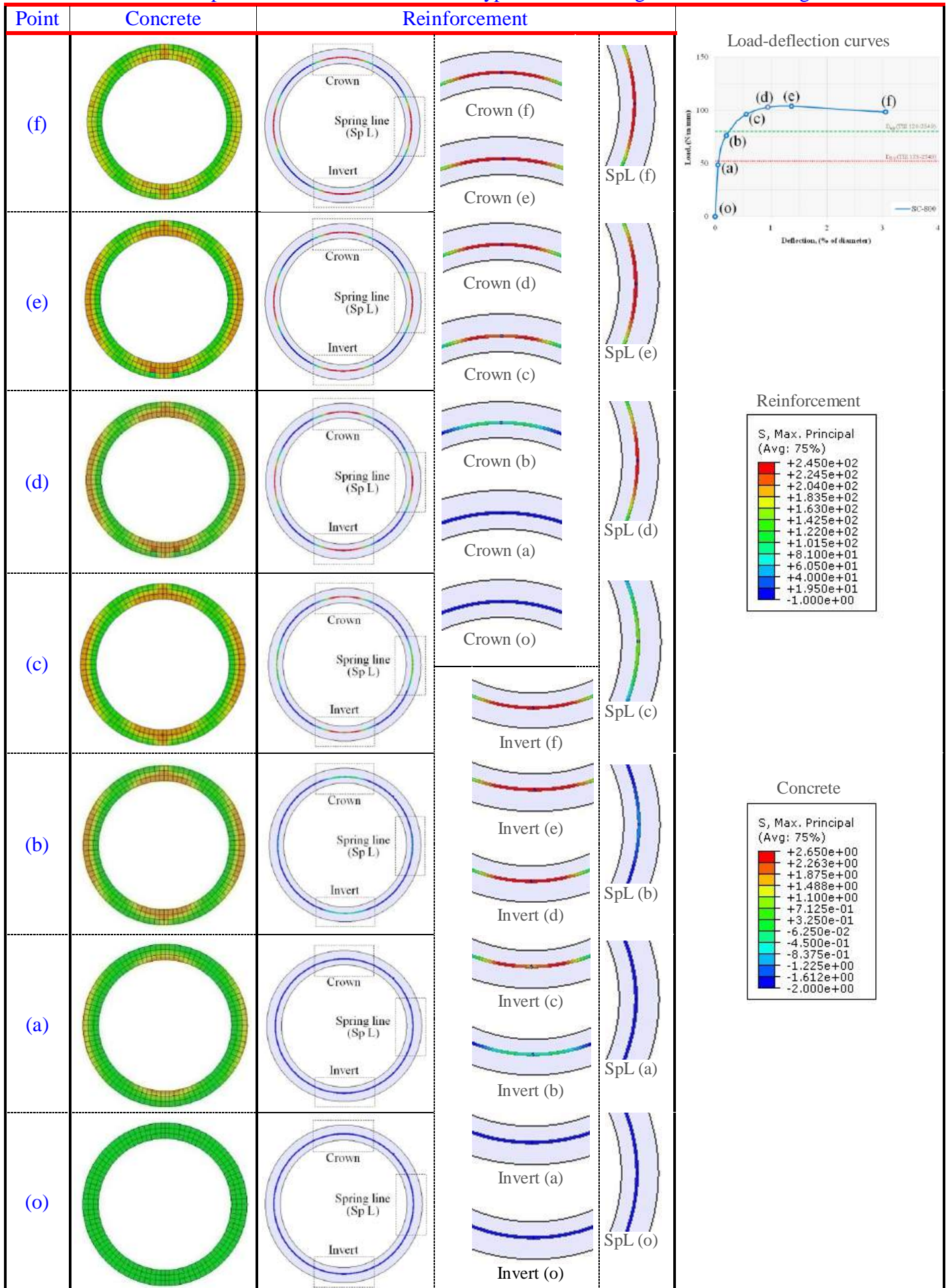


Table 7: Development of stress distribution for typical SE-800 single elliptical steel cage model

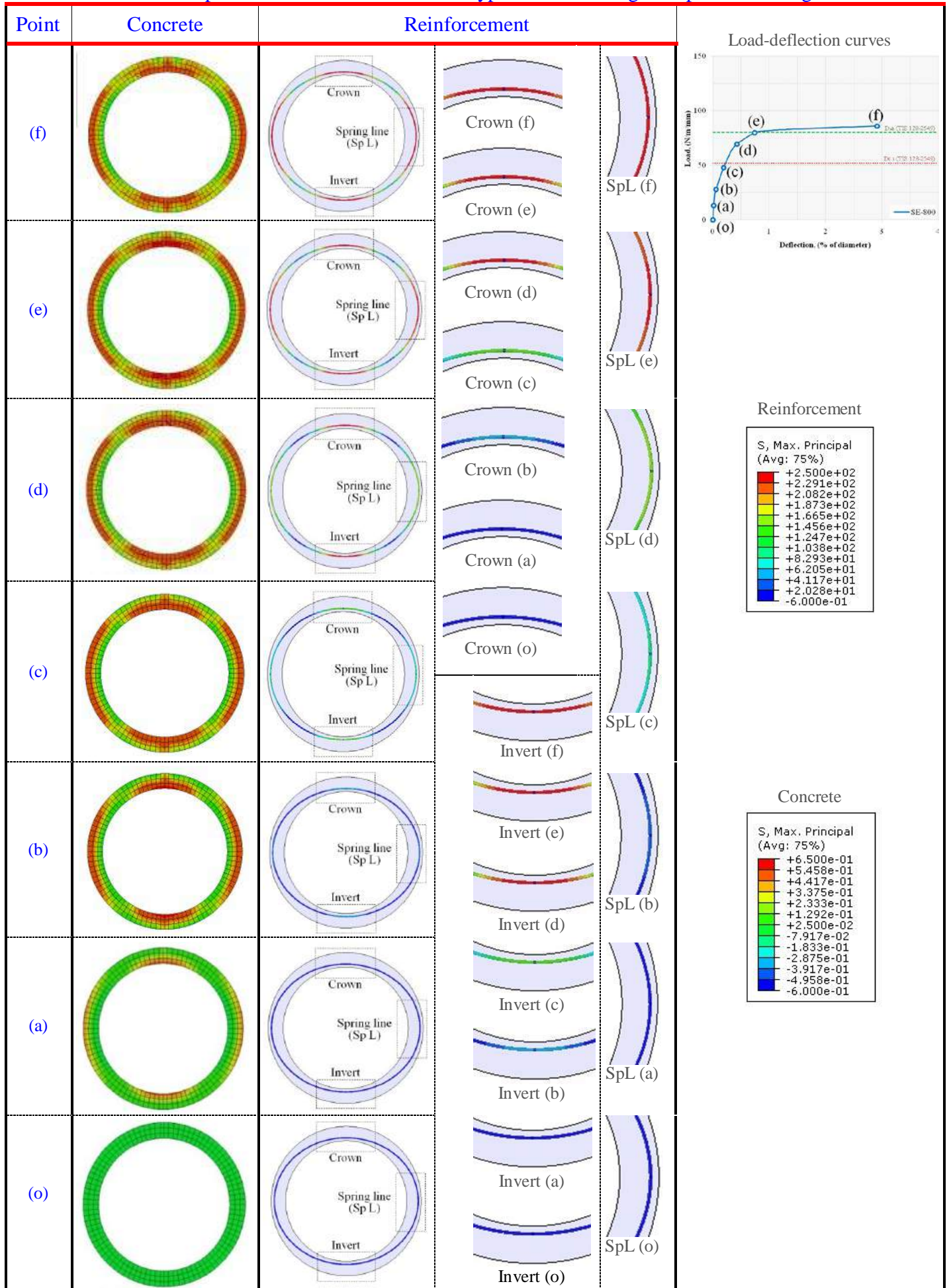


Table 8: Development of stress distribution for typical DC-1000 double circular steel cage model

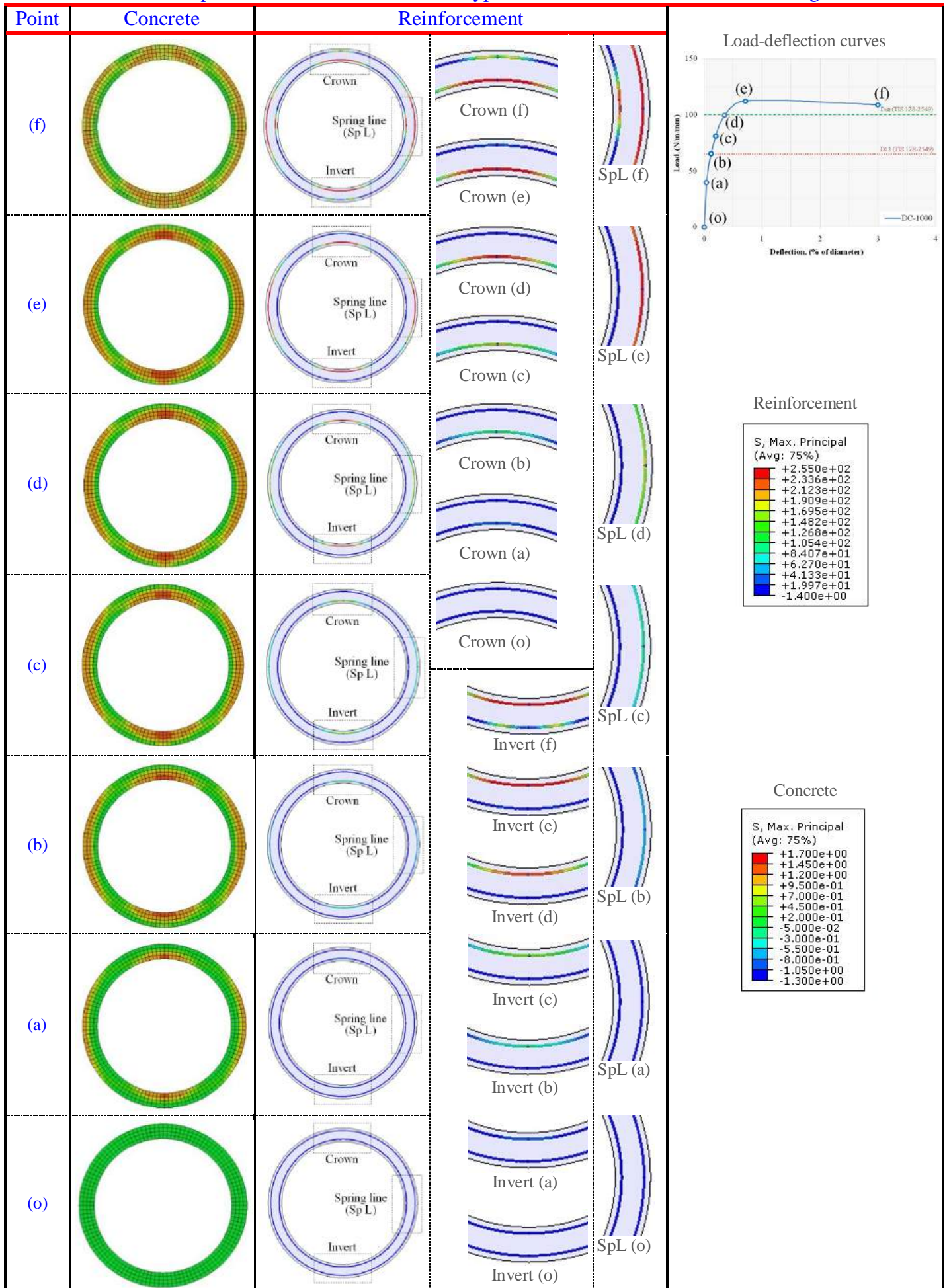
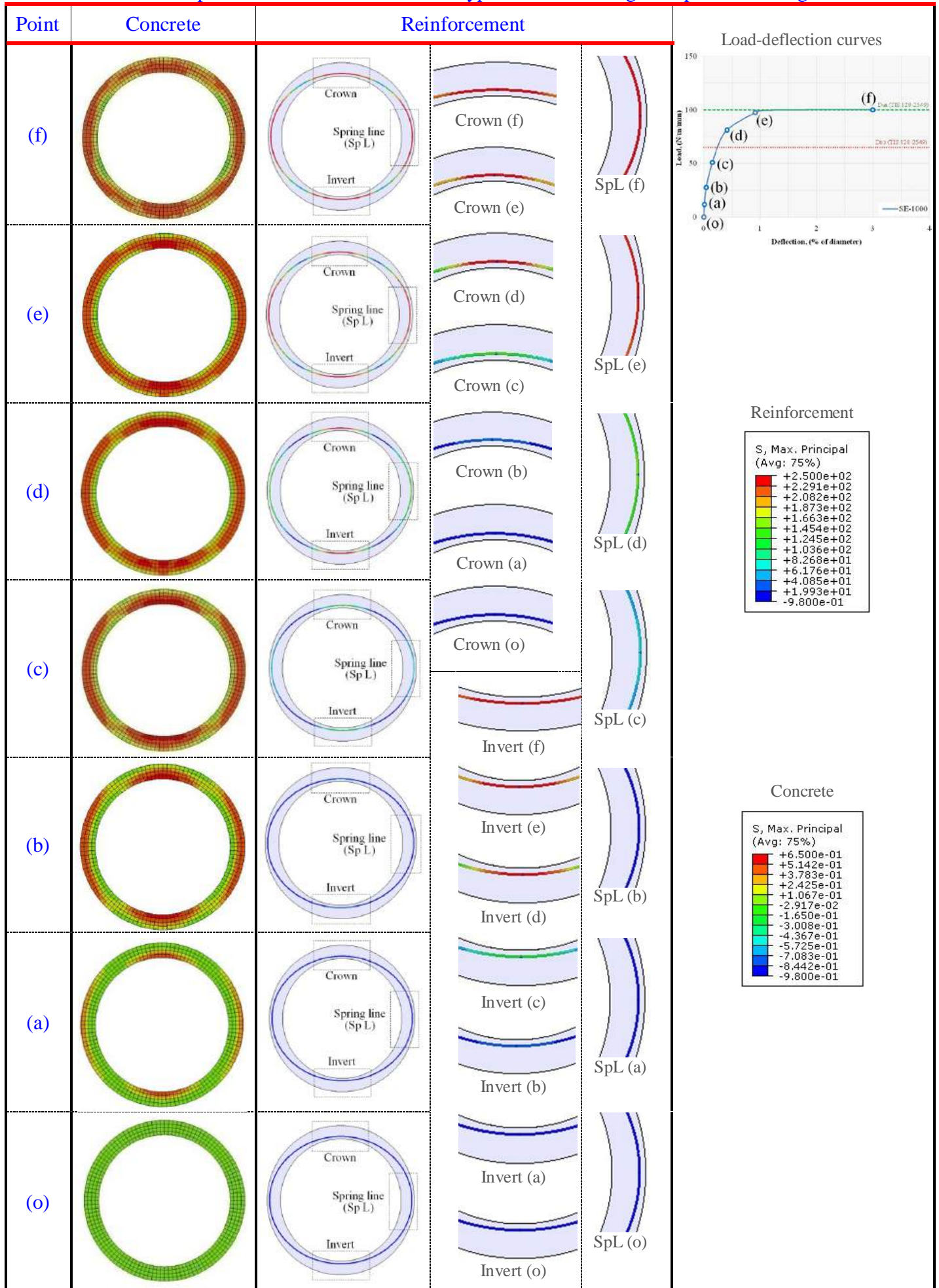


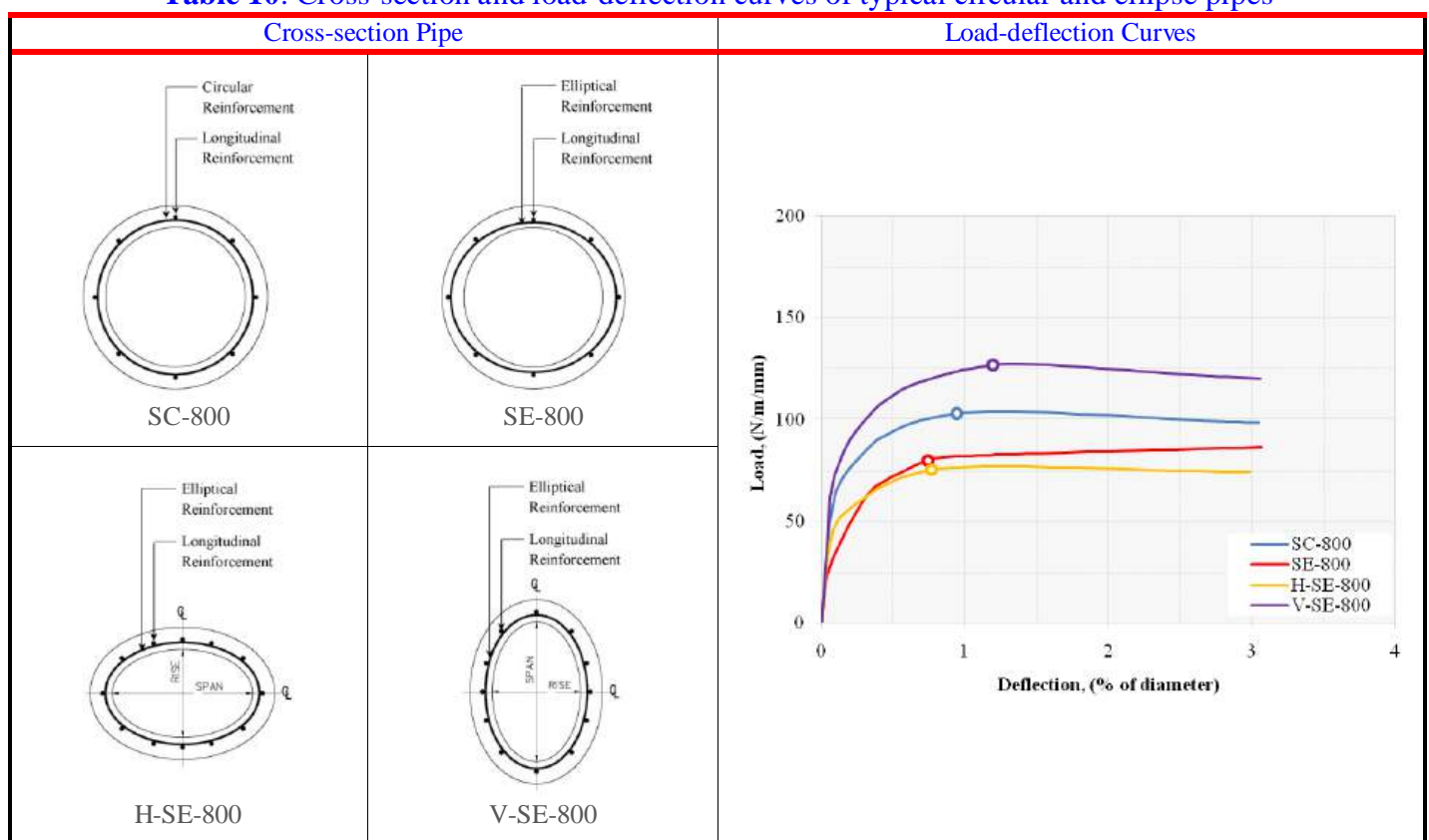
Table 9: Development of stress distribution for typical SE-1000 single elliptical steel cage model



6.2 Comparison between Circular and Elliptical Pipes

For the second category, two sets of the load-deformation curves and the corresponding stress development across the sections of the RCP are compared. The first set (Tables 10 and 11) are the finite element results obtained from four RCP, each of which contains a single steel cage. These include (1) the circular pipe with a single circular cage SC-800, (2) the circular pipe with a single elliptical cage SE-800, and the elliptical pipes with a single elliptical cage with either (3) horizontal position H-SE-800, or (4) vertical position V-SE-800. The second set, shown in Tables 12 and 13, are the results obtained from four RCP, which are (1) the circular pipe with double circular cage DC-1000, (2) the circular pipe with single elliptical cage SE-1000, and the elliptical pipes with double elliptical cages with either (3) horizontal position H-DE-800, or (4) vertical position V-DE-800. For each set of comparisons, each pipe contains the same cross-sectional area.

Table 10: Cross-section and load-deflection curves of typical circular and ellipse pipes



Tables 10 and 12 show similar behavior but different in magnitude for the load-deflection curves of both circular and elliptical shapes of the RCP with an equivalent cross-sectional area. However, for each set of curves, the elliptical pipe with a vertical position indicates the highest ultimate load capacity compared with the remaining ones. The highest load-carrying capability takes advantage of the longest depth of the compressive stress diagram above the neutral axis of the cross-section affecting the flexural behavior. This results in the longest moment arm of the resisting moment developed at any cross-sectional area of these vertical elliptical RCP. The comparison between the SC-800 and SE-800 in Table 10, however, provides an unexpected magnitude. This may cause by the calibration of their parameters, which are based on the different works of literature. Future study is suggested to investigate the appropriate values of these

parameters, especially the sensitive tensile strength of the concrete.

Tables 11 and 13 present some stress distribution for concrete and steel including the deformed shapes obtained from the TEB test of the finite element models of these circular and ellipse pipes. Results from the investigation are similar to the ones obtained from the first category.

Table 11: Stress distribution and deformed shape for typical circular and ellipse pipes

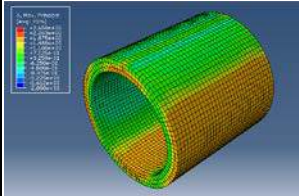
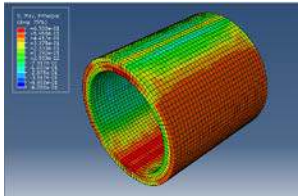
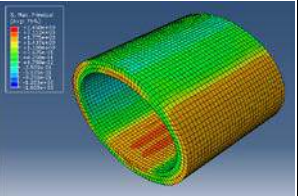
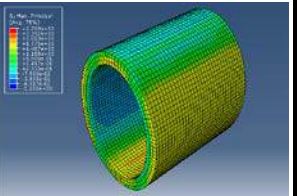
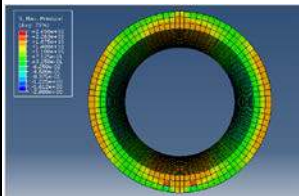
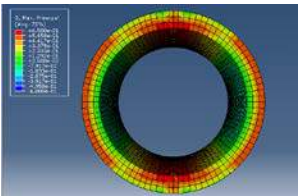
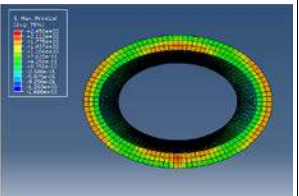
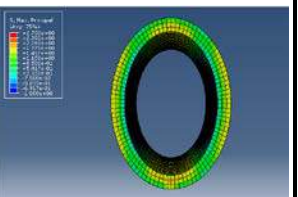
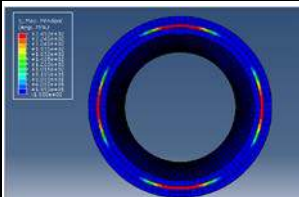
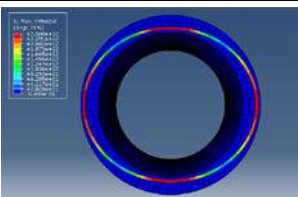
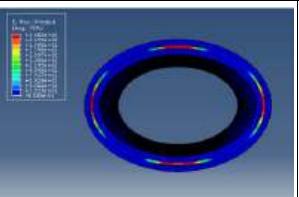
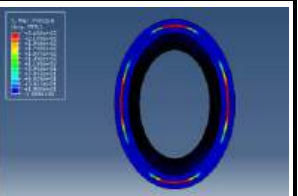
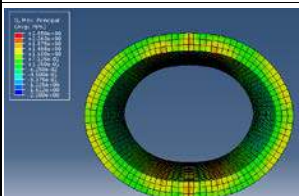
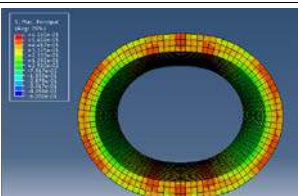
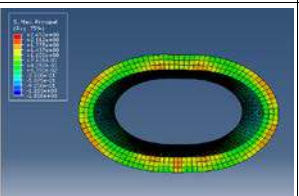
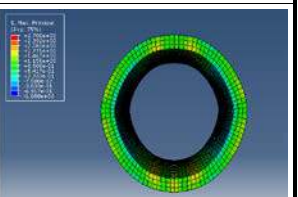
Model	SC-800	SE-800	H-SE-800	V-SE-800
Concrete (Isometric view)				
Concrete				
Reinforcement (Scale factor 2.5)				
deformed shape (Scale factor 2.5)				

Table 12: Cross-section and load-deflection curves of typical circular and ellipse pipes

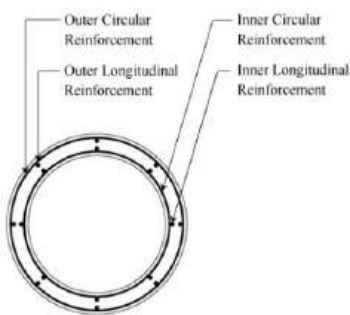
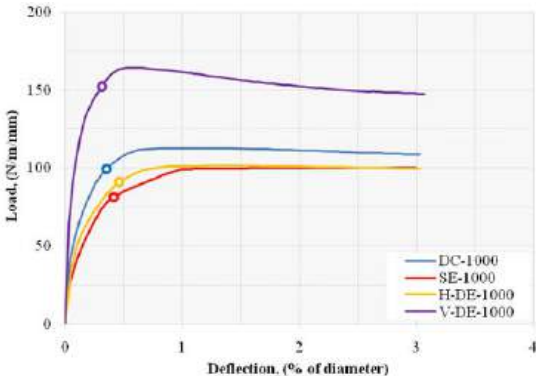
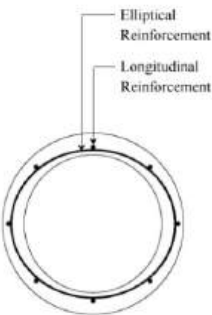
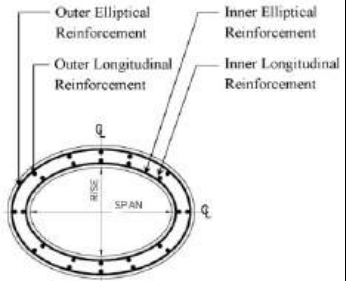
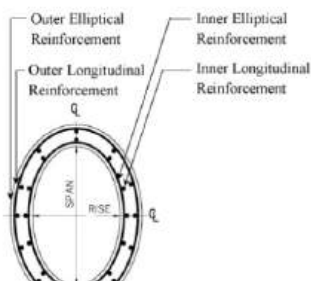
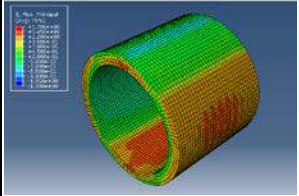
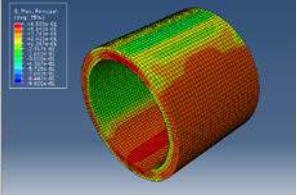
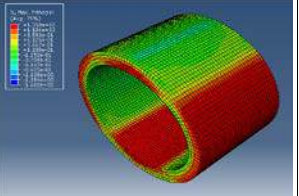
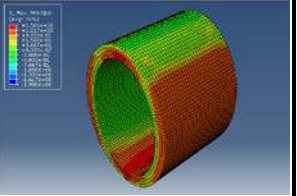
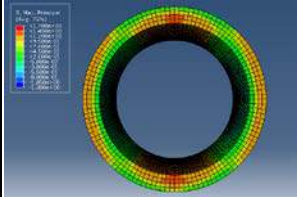
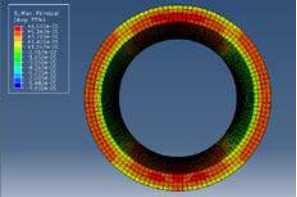
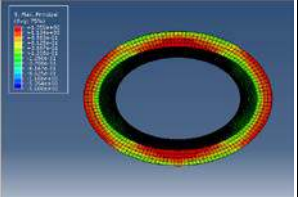
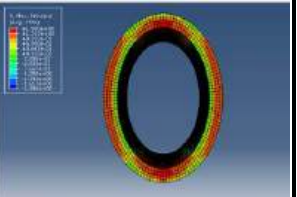
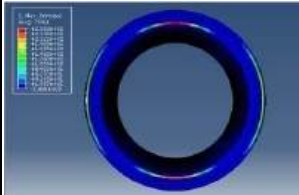
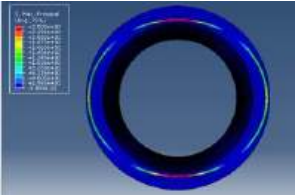
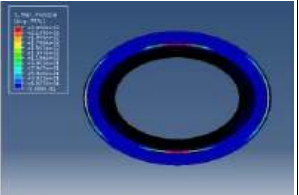
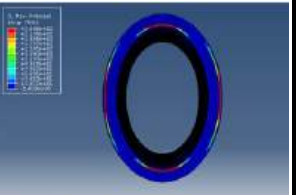
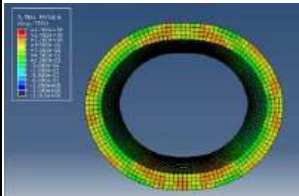
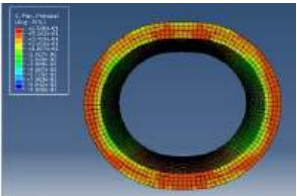
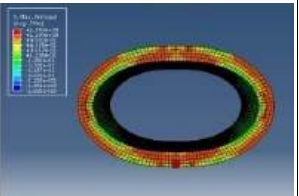
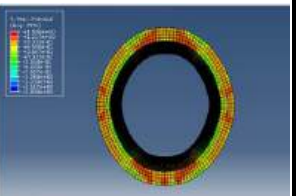
Cross-section Pipe	Load-deflection Curves
 <p>DC-1000</p>	
 <p>SE-1000</p>	
 <p>H-DE-1000</p>	
 <p>V-DE-1000</p>	

Table 13: Stress distribution and deformed shape for typical circular and ellipse pipes

Model	DC-1000	SE-1000	H-DE-1000	V-DE-1000
Concrete (Isometric view)				
Concrete				
Reinforcement (Scale factor 2.5)				
deformed shape (Scale factor 2.5)				

7 Conclusion

To simulate the TEB test of the RCP model using ABAQUS software, three different material properties for the three main components are defined. This includes the concrete pipe, the steel cage, and the (upper & lower) bearing strips. The behavior of the longitudinal bearing strips is simply defined by using the material properties of wood. The material properties of the steel cage of the RCP model are simulated as an elastic-plastic behavior. The concrete damaged plasticity (CDP) model is selected to represent the material property of concrete. The algorithms presented in the literature are applied to develop the information obtained from the inelastic compressive and tensile stress-strain diagram for creating the CDP material model.

The behavior of the RCP subjected to static loading conditions using the Finite Element model of ABAQUS software is divided into two categories. The first category investigates the pipes of circular cross-sections with different types of steel cages. The second category compares the circular pipes with either circular or elliptical cages and the elliptical pipes with elliptical cages.

For the first category, the pipes of circular cross-section include the single circular, the double circular, and the elliptical steel cages. Under the TEB test simulation, the RCP behaves like a vertical ring under a downward loading. This behavior is similar to those results found in the literature. The vertical pipe diameter tends to be decreased while the horizontal diameter tends to be increased. Therefore, at the crown, the compressive and tensile stresses are produced above and below the neutral axis of the pipe wall, respectively. At the invert, however, the compressive and tensile stresses are created below and above the neutral axis of the pipe wall, respectively. At the

spring line level, compressive and tensile stresses are produced inward and outward in the radial directions from the neutral axis of the pipe wall. The stress development both in concrete and reinforcing steel is presented in a systematic sequence. This reveals the redistribution process from concrete to reinforcing steel. As the applied load is continuously increased, the excessive principal stress, which is larger than the concrete capability, is transferred to the reinforcing steel cage, which can experience a higher magnitude of stress until the structure is reached its ultimate failure.

For the second category, the circular pipes consisting of either circular or elliptical steel cages are compared with the elliptical pipes consisting of elliptical steel cages. Two sets of the investigation are proposed. In the first set, each RCP contains a single steel cage. However, in the second set, the circular pipes include either double circular or single elliptical steel cages, while the elliptical pipes include double elliptical cages. In addition, the elliptical pipes are considered in both horizontal, and vertical positions. For each set of comparisons, each pipe contains the same cross-sectional area. The load-deflection curves obtained from the circular and elliptical RCP for both sets provide similar behavior but their magnitudes are different. For each set of curves, the elliptical pipe with a vertical position provides the highest ultimate load capacity. This is caused by the longest moment arm of the resisting moment developed at any cross-sectional area of these vertical elliptical RCP. Additional results, such as the stress distribution for concrete and steel including the deformed shapes, of these circular and ellipse pipes from the investigation are similar to those obtained from the first category.

8 Availability of Data and Material

Data can be made available by contacting the corresponding authors.

9 References

- Abaqus. (2013). *Abaqus 6.13 Analysis User's Guide Volume III: Materials*. Dassault Systèmes Simulia. http://130.149.89.49:2080/v6.13/pdf_books/ANALYSIS_3.pdf
- Alfarah, B., López-Almansa, F., & Oller, S. (2017). New Methodology for Calculating Damage Variables Evolution in Plastic Damage Model for RC Structures. *Engineering Structures*, 132, 70-86. DOI: 10.1016/j.engstruct.2016.11.022
- American Concrete Pipe Association. (2011). *Concrete Pipe Design Manual*. <http://resources.concretepipe.org/concrete-pipe-design-manual>
- American Concrete Pipe Association. (2020). *Post Installation Evaluation and Repair of Installed Reinforced Concrete Pipe*. <https://www.concretepipe.org/pipe-box-resources/inspection/post-installation/>
- ASTM. (2018). ASTM C76-16: Standard Specification for Reinforced Concrete Culvert, Storm Drain, and Sewer Pipe. West Conshohocken, PA: ASTM
- Atichat, A., Sirimontree, S., & Witchayangkoon, B. (2017). Behaviors of Concrete Beam to Column Connections under Static Load Using Finite Element Method. *International Transaction Journal of Engineering Management & Applied Sciences & Technologies*, 8(2), 57-67. <https://tuengr.com/Vol82.html>
- Buda-Ozóg, L., & Skrzypczak, I. (2015). Experimental and Numerical Analysis of Cracks in the Reinforced Concrete Pipes. *Journal of Civil Engineering, Environmental and Architecture*, 62(3), 63-74.
- CSA A257-14. (2014). Standards for Concrete Pipe and Manhole Sections. Mississauga, ON: CSA.
- da Silva, J. L., El Debs, M. K., & Kataoka, M. N. (2018). A Comparative Experimental Investigation of Reinforced-Concrete Pipes under Three-Edge-Bearing Test: Spigot and Pocket and Ogee Joint Pipes. *Acta*

- Doru, Z. (2017). Steel Fibers Reinforced Concrete Pipes-Experimental Tests and Numerical Simulation. *IOP Conference Series: Materials Science and Engineering*, 245(2), 022032. DOI: 10.1088/1757-899X/245/2/022032
- Erdogmus, E., & Tadros, M. K. (2006). Behavior and Design of Buried Concrete Pipes. *Nebraska Department of Transportation Research Reports*, 54. <http://digitalcommons.unl.edu/ndor/54>
- Ferrado, F. L., Escalante, M. R., & Rougier, V. C. (2016). Numerical Simulation of the Three Edge Bearing Test of Steel Fiber Reinforced Concrete Pipes. *Mecánica Computacional*, 34(34), 2329-2341. <http://venus.santafe-conicet.gov.ar/ojs/index.php/mc/article/view/5156>
- Michał, S., & Andrzej, W. (2015). Calibration of the CDP model parameters in Abaqus. World Congr. Adv. Struct. Eng. Mech. (ASEM15), Incheon Korea.
- Mohamed, N., & Nehdi, M. L. (2016). Rational Finite Element Assisted Design of Precast Steel Fibre Reinforced Concrete Pipes. *Engineering Structures*, 124, 196-206. DOI: 10.1016/j.engstruct.2016.06.014
- Montha, A., Sirimontree, S., & Witchayangkoon, B. (2018). Behaviors of the Composite Slab Composed of Corrugated Steel Sheet and Concrete Topping Using Nonlinear Finite Element Analysis. *International Transaction Journal of Engineering, Management, & Applied Sciences & Technologies*, 9(2), 75-84. <https://tuengr.com/Vol91.html#V92>
- Ontario Concrete Pipe Association. (n.d.). *OCPA Concrete Pipe Design Manual*. <https://ccppa.ca/design/>
- Ramadan, A., Shehata, A., Younis, A-A., Wong, L. S., & Nehdi, M. L. (2020). Modeling Structural Behavior of Precast Concrete Pipe with Single Elliptical Steel Cage Reinforcement. *Structures*, 27, 903-916.
- Riahi, E. (2016). *Evaluation of Structural Capacity of Epoxy-Coated Concrete Pipes and Its Interaction with Soil*. Doctoral dissertation, the University of Texas at Arlington. <https://rc.library.uta.edu/uta-ir/handle/10106/27873>
- Tehrani, A. D. (2016). *Finite Element Analysis for ASTM C-76 Reinforced Concrete Pipes with Reduced Steel Cage*. Master's Thesis, the University of Texas at Arlington. DOI: 10.13140/RG.2.2.13688.08967
- TIS. (2000). *Thai Industrial Standards: Steel Bars for Reinforced Concrete: Round Bars*. TIS.20-2543, Thai Industrial Standards Institute, Ministry of Industry, Thailand.
- TIS. (2006). *Thai Industrial Standards Precast Reinforced Concrete Drainage Pipe*. TIS.128-2549, Thai Industrial Standards Institute, Ministry of Industry, Thailand.
- Wen, Q-J., Jing, H-W., Sanda, S., & Zhuan, S-S. (2017). Experimental Investigation of Mechanical Properties of Centrifugal Concrete in Circular Pipes. *Journal of Materials in Civil Engineering*, 29(4), 04016251. DOI: 10.1061/(asce)mt.1943-5533.0001771
- Wong, L. S., & Nehdi, M. L. (2018). Critical Analysis of International Precast Concrete Pipe Standards. *Infrastructures*, 3(3), 18. DOI: 10.3390/infrastructures3030018
- Younis, A-A., Shehata, A., Ramadan, A., Wong, L. S., & Nehdi, M. L. (2021). Modeling Structural Behavior of Reinforced-Concrete Pipe with Single, Double and Triple Cage Reinforcement. *Engineering Structures*, 240, 112374. DOI: 10.1016/j.engstruct.2021.112374



Narongsak Kosaiyakanon is a Master's Candidate of Civil Engineering at Thammasat University, Thailand. He received his Bachelor of Engineering degree in Civil Engineering from Prince of Songkhla University, Thailand. He works at the Department of Rural Roads, Ministry of Transport, Thailand. He is interested in Design Buildings and Bridges.



Dr. Chaisak Pisitpaibool is an Assistant Professor at the Department of Civil Engineering, Thammasat University. He received his B.Eng. and M.Eng. from Khon Khaen University. He was a Lecturer at Chiang Mai University. He got a PhD from Nottingham University, UK. His research encompasses Prestress Engineering.